Supporting Information

Ultrasensitive 1D field-effect phototransistor: $CH_3NH_3PbI_3$ nanowire sensitized individual carbon nanotube

*M. Spina[1], B. Náfrádi[1], H. M. Tóháti[2], K. Kamarás[2], E. Bonvin[1], R.Gaal[1], L. Forró[1], E. Horváth[1]**

Estimation of the charge carrier mobility

The hole mobilities of CNT-FETs were extracted from the linear region of the transfer characteristics using the expression for the low-field field-effect mobility

$$\mu = \frac{dI_D}{dV_G} \frac{L}{WC_iV_D} \qquad \text{(Equation 1)}$$

where C_i is the capacitance of the gate insulator ($= \varepsilon_0\varepsilon_r/d = 1.64\ 10^4\ Fm^{-2}$).

Transfer characteristic in the light induced off state

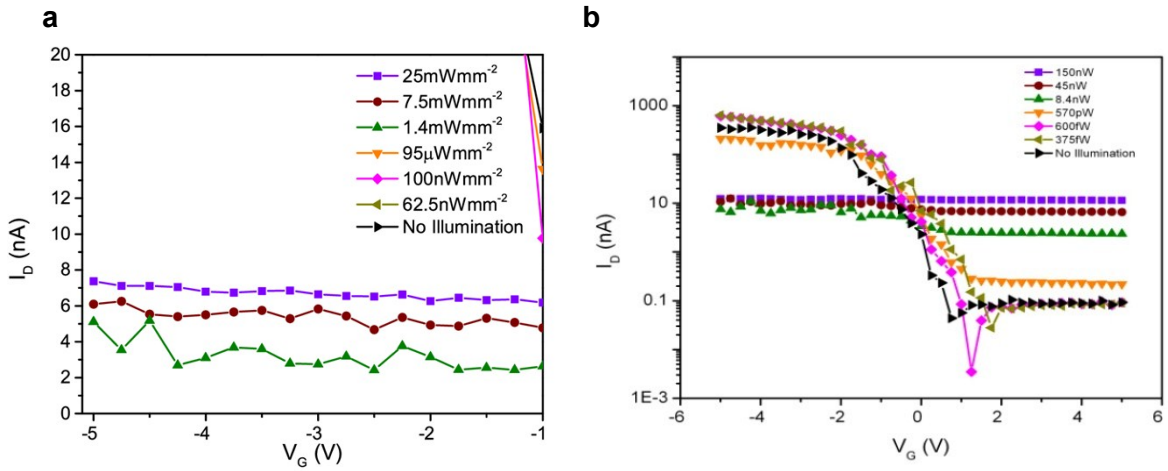

Figure S1. Transfer characteristic of the hybrid phototransistor presented in the main text. a) The transfer characteristic is shown upon different high light irradiation intensities in the electrostatic ON-state. b) The same data is presented in logarithmic scale to emphasize the monotonous increase of the photocurrent with light intensity in the electrostatic ON-state.

Transfer Characteristics of additional Hybrid Devices

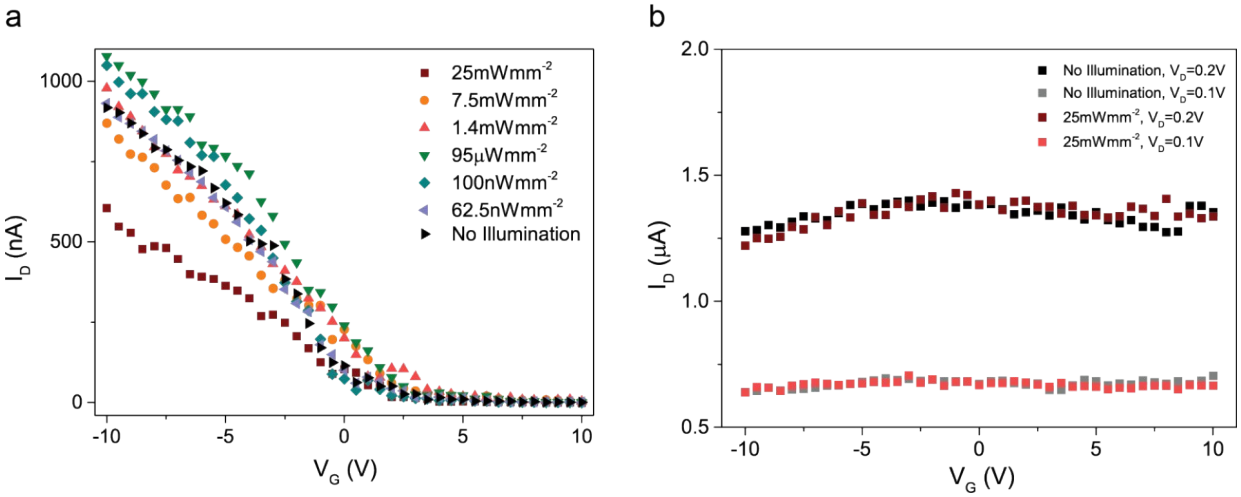

Figure S2. Transfer characteristic of a semiconducting (a) and a metallic (b) CNT-FET/MAPbI$_3$NW hybrid device.

An additional semiconducting hybrid device was characterized under the same experimental conditions as the one described in the main text. The photo-induced charge modulation (both positive and negative) was also recorded, with the difference that the number of scattering centers generated was not enough to completely switch off the channel (Figure S2a).

Moreover, an individual metallic nanotube was also sensitized with the perovskite nanowires but in this case no photocurrent was observed (Figure S2b).

Infrared and Raman spectroscopy

Depositing the $CH_3NH_3PbI_3$ nanowires affected only the IR, but not the Raman spectra of the CNT Buckypaper films. As the strong resonance Raman lines of the nanotubes dominate the spectra over molecular vibrations (Figure S3), information on chemical transformation is drawn from the D/G peak ratio. Chemical functionalization should result in the increase of this ratio; the lack of such increase indicates that little, if any, change in the bonds attached to the tube walls occurred. Charge transfer, *i.e.* doping of the tubes would cause an overall decrease in all peak intensities; however, such a change is difficult to observe because of the relative nature of the measurement (all spectra are normalized to the G peak) and the necessity of baseline correction due to the strong $MAPbI_3$ luminescence. Such subtle effects in the electronic structure show up much more clearly in the IR/NIR spectra.

After initial deposition of the nanowires, infrared-active vibrations of $MAPbI_3$[1] appeared (Figure S4) but the S_{11} electronic transition of the carbon nanotubes was not affected (Figure S5). Significant changes happened on illumination, as shown in Figure S5. The quantity derived from the measured transmittance, *T*, is

$$\Delta A = \frac{T_{dark} - T_{illum}}{T_{dark}}, \qquad \text{(Equation 2)}$$

the change in absorption due to illumination. This change consists of an increase in the low-frequency absorption, together with a decrease in the S_{11} transition, indicative of charge transfer[2]. Most of the increase is observed in the first 10 minutes of illumination, but it is continuous up to about 35 minutes. The effect is reversible, although relaxation to the original state after switching off the light is slower.

Raman spectra

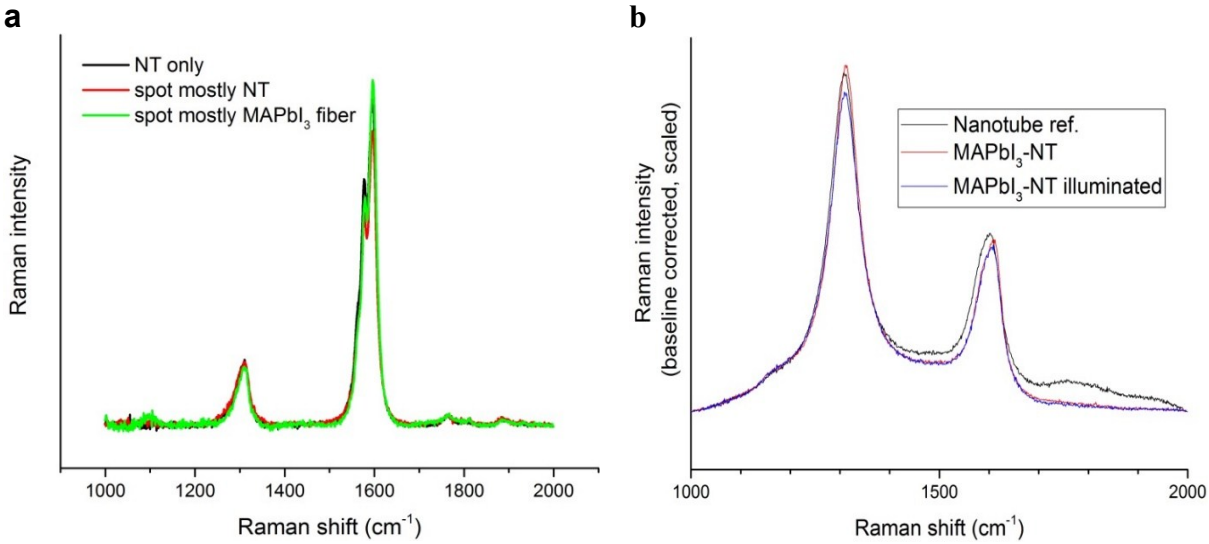

Figure S3 (a) Raman spectra of mixed single-walled nanotubes before and after treatment with $MAPbI_3$. Spectra taken close to the $MAPbI_3$ fibers and at untreated parts of the sample did not show significant difference in D/G ratio. Spectra are normalized to the G band.
(b) Raman spectra of mixed multi-walled nanotubes before and after treatment with $MAPbI_3$, and after illumination with 633 nm light. Neither treatment with $MAPbI_3$ fibers nor illumination resulted in any significant change in D/G ratio. Spectra are normalized to the G band.

Infrared Spectra

Below we compare the infrared spectra of $MAPbI_3$ pristine nanowires with those of the hybrid structures formed by $MAPbI_3$NW and CNT films. Adhesion to the surface splits some lines in the $MAPbI_3$ spectrum. The nanowire spectra were recorded in diffuse reflectance (DRIFT) mode, all others were calculated from transmission.

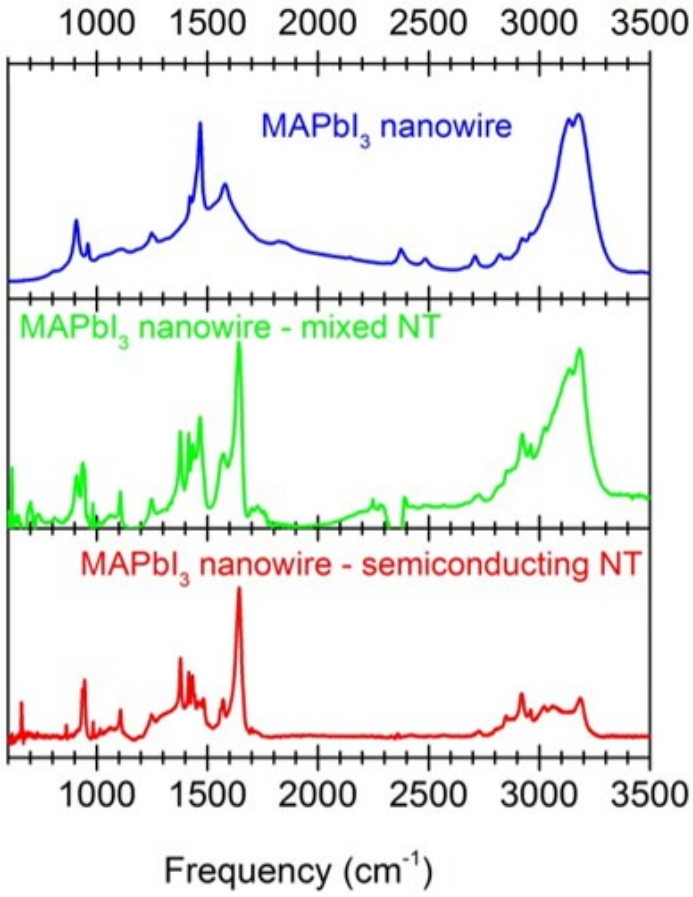

Figure S4 Infrared spectra of $MAPbI_3$ as-prepared nanowire, and hybrids from both mixed and semiconducting single-walled nanotube films. Absorption was calculated from diffuse reflectance (DRIFT) for nanowires and from transmission in all other cases. Baseline correction was applied to absorbance spectra.

Changes in infrared spectra upon illumination

Based on the IR spectra below we compare the change of a $MAPbI_3$-semiconducting CNT hybrid to that of the pristine nanotube sample after 10 minutes of illumination. The hybrid structure shows the effects of nanotube doping (explained in the DOS illustrations for electron doping): increase in the low-frequency free-carrier absorption and decrease of the S_{11} transition intensity due to filling of final states.

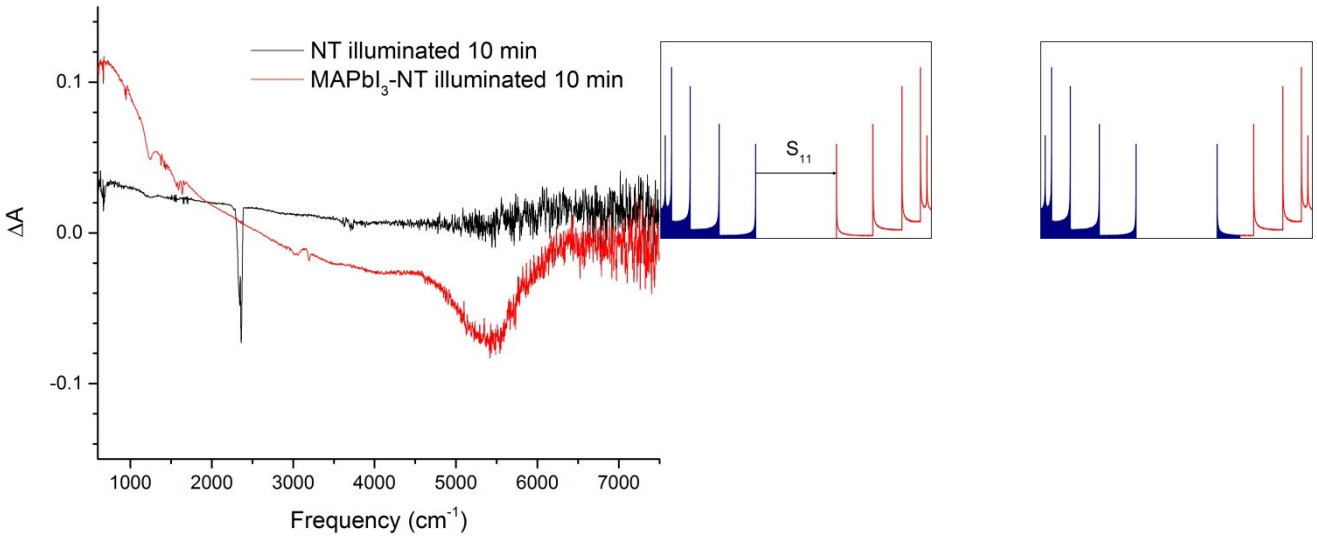

Figure S5 Change in absorption upon 10 minutes illumination by 633 nm light of a semiconducting nanotube film (black curve) and a $MAPbI_3$-semiconducting SWNT hybrid (red curve). The red curve clearly shows the effects of added carriers into the CNT (illustrated on the right). The sharp peaks in the nanotube spectrum are due to atmospheric carbon dioxide.

Photocurrent spectroscopy

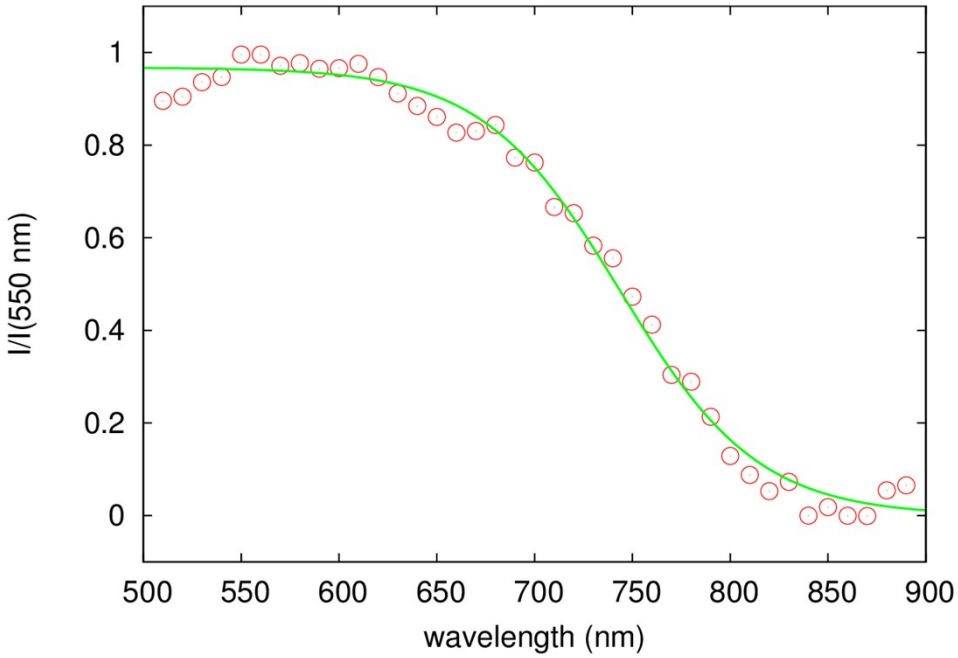

Figure S6 Spectral sensitivity of a CNT-$MAPbI_3$ device at room temperature. The line is a fit to the Fermi-Dirac distribution. The spectral sensitivity rapidly increases below 780 nm characteristic to $MAPbI_3$.

Scanning electron microscopy on individual carbon nanotube FETs

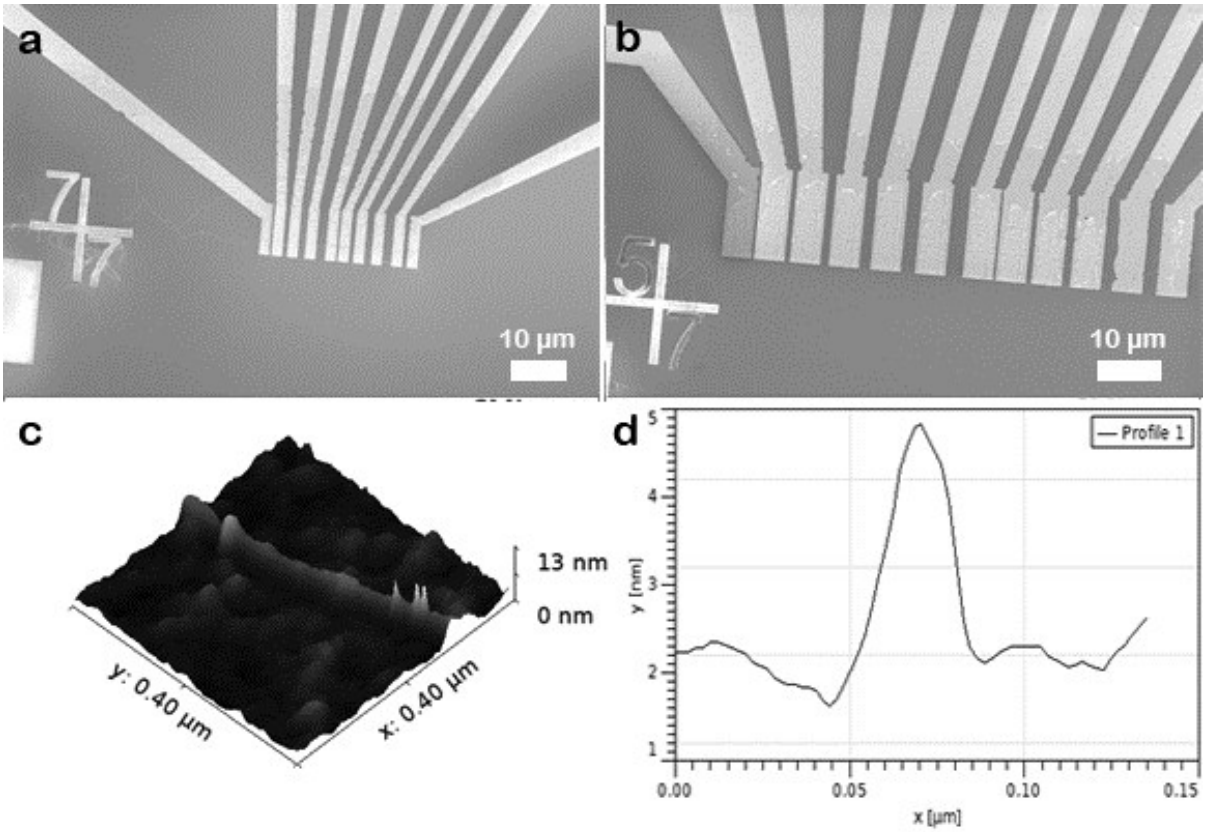

Figure S7 Top: High resolution SEM micrographs of individual carbon nanotube FETs. Bottom: 3D reconstruction of the AFM of the individual CNT-FET and an AFM cross section showing the individual CNT.

Highly linear gain of $MAPbI_3$NW/CNT-FEpT facilitates detector applications.

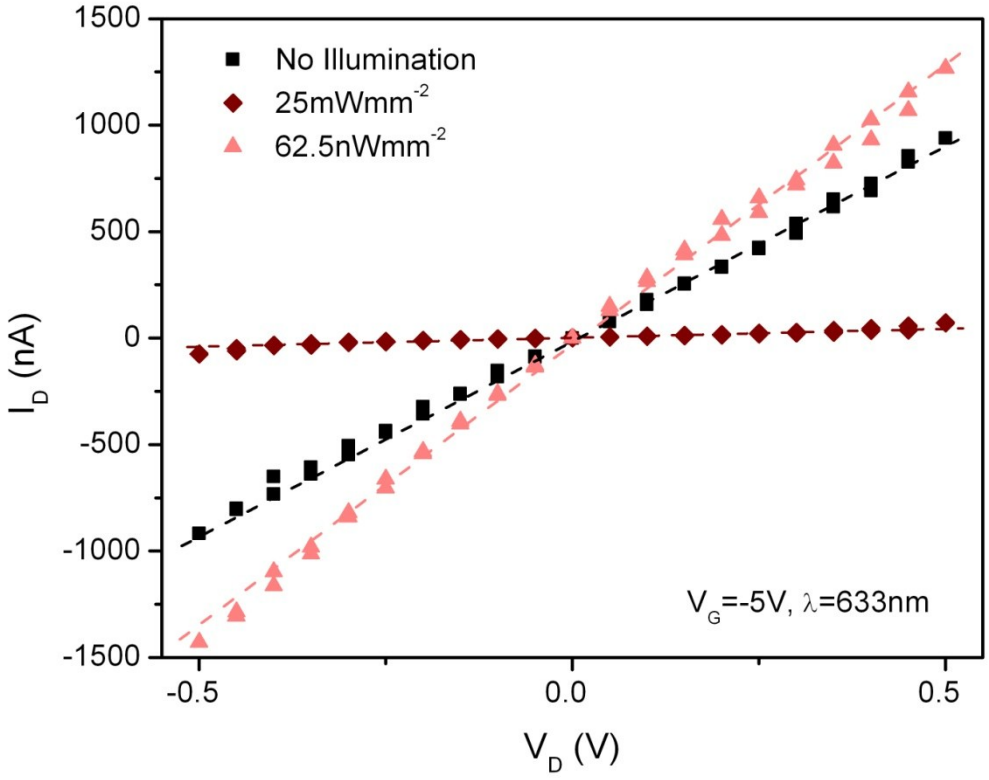

Figure S8 I_D-V_D curve of the $MAPbI_3$NW/CNT-FEpT shows a highly linear gain as a function of V_G

Photoresponsivity of the pristine individual CNT-FET

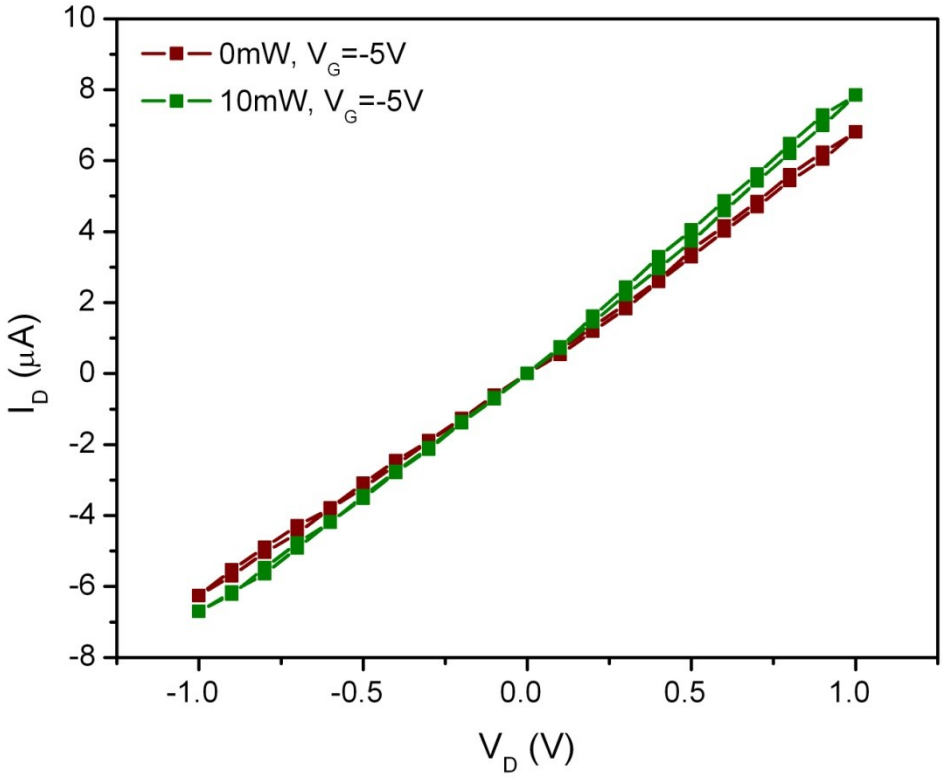

Figure S9: The illumination dependence of the transfer characteristics of the pristine individual CNT-FET. The maximum responsivity at V_D=1 V is R=1×10^{-4} A/W.

References

1 Horváth, E. *et al.* Nanowires of Methylammonium Lead Iodide (CH3NH3PbI3) Prepared by Low Temperature Solution-Mediated Crystallization. *Nano Letters* **14**, 6761-6766, doi:10.1021/nl5020684 (2014).

2 Borondics, F. *et al.* Charge dynamics in transparent single-walled carbon nanotube films from optical transmission measurements. *Physical Review B* **74**, 045431 (2006).